Overexpression of the *WAPO-A1* gene increases the number of spikelets per spike in bread wheat

Lukas M. Wittern[1†], Jose M. Barrero[4†], William D. Bovill[4], Klara L. Verbyla[4], Trijntje Hughes[4], Steve M. Swain[4], Gareth Steed[1], Alex A.R. Webb[1], Keith Gardner[3], John Jacobs[2], Claus Frohberg[2], Ralf-Christian Schmidt[2], Colin Cavanagh[5], Antje Rohde[2], Mark Davey[2‡] and Matthew A. Hannah [2‡*]

[1]Department of Plant Sciences, University of Cambridge, CB2 3EA, UK

[2]BASF, BBCC - Innovation Center Gent, Technologiepark 101, 9052 Ghent, Belgium

[3]National Institute of Agricultural Botany (NIAB), Huntingdon Road, Cambridge, CB3 0LE, UK

[4]Commonwealth Scientific and Industrial Research Organisation, Agriculture and Food, Black Mountain Science and Innovation Park, Canberra, ACT 2601, Australia

[5]BASF Australia Ltd., 28 Freshwater Place, 3006 Melbourne, Australia

† Shared first authors
‡ Shared last authors
*Corresponding author. Email: matthew.hannah@basf.com, Tel: +3292508598

Abstract

Two homoeologous QTLs for number of spikelets per spike (SPS) were mapped on chromosomes 7AL and 7BL using two wheat MAGIC populations. Sets of lines contrasting for the QTL on 7AL were developed which allowed for the validation and fine mapping of the 7AL QTL and for the identification of a previously described candidate gene, *WHEAT ORTHOLOG OF APO1* (*WAPO1*). Using transgenic overexpression in both a low and a high SPS line, we provide a functional validation for the role of this gene in determining SPS also in hexaploid wheat. We show that the expression levels of this gene positively correlate with SPS in multiple MAGIC founder lines under field conditions as well as in transgenic lines grown in the greenhouse. This work highlights the potential use of *WAPO1* in hexaploid wheat for further yield increases. The impact of *WAPO1* and SPS on yield depends on other genetic and environmental factors, hence, will require a finely balanced expression level to avoid the development of detrimental pleiotropic phenotypes.

Keywords: *WAPO1*, spikelets per spike (SPS), spike architecture, Multiparent Advanced Generation Intercross (MAGIC), wheat transgenics

Introduction

Grain yield is a highly complex trait which is the product of a network of inter-connected yield-component traits, such as tiller number, inflorescence architecture and the rate of grain filling, often with interdependencies and trade-offs involved[1]. Studying individual yield-component traits, particularly those with higher heritability such as spikelet number per spike (SPS)[2] can assist in reducing some of this complexity. As spikelets are specialized branches that produce grains, breeding for increased SPS could increase grain yield by increasing grain number and sink capacity.

SPS is affected by genes affecting flowering time through vernalization, photoperiod or earliness *per se (eps)* pathways: *VRN1*, *FUL2*, *FUL3*, *PPD1*, *VRN3*/*FT1*, *FT2*, *ELF3*[3–7]. Spring or winter growth habit is determined primarily by variation in the *VRN* genes. *PPD1* controls photoperiod-dependent floral induction, with the photoperiod insensitive allele *PPD-D1a* accelerating flowering, whilst *ELF3* is a minor effect *eps* gene. However, identification and characterization of major effect genes that increase SPS independently of these pathways has been limited so far.

The genetic dissection of grain yield and yield-component traits in hexaploid wheat is complicated by the compensatory effects of homoeologous genes. Their analysis in diploid model plants, such as rice, usually reveal QTLs with much higher effect sizes, e.g. 20-40% in rice vs 2-9% in hexaploid wheat[8]. Previous rice studies identified several genes involved in the regulation of panicle size and grain number and thus their orthologs provide a basis for studies in other cereals[9]. The rice gene *ABERRANT PANICLE ORGANIZATION 1* (*OsAPO1)* regulates panicle size, grain number[10,11] and yield[12,13] and higher expression of the *OsAPO1* transcript leads to more primary branches[11]. *OsAPO1* is syntenic with a major wheat SPS Quantitative Trait Locus (QTL) on chromosome 7AL in several bi-parental mapping populations and diversity panels[2,14–21] as well as a minor homoeologous QTL on 7BL[22,23].

More recently the *WHEAT ORTHOLOGUE OF APO1 (WAPO1)* has been proposed as the candidate gene for the SPS QTL on 7AL by multiple authors[24–26], and validated in tetraploid wheat using a combination of mutants and transgenic lines[27]. However, transgenic overexpression in multiple backgrounds of hexaploid wheat has not yet been reported, limiting our understanding of gene function, effect size, and pleiotropic effects for the more relevant hexaploid wheat breeding.

Multi-parental Advanced Genetic Inter-Crossed (MAGIC) populations are well suited for QTL mapping due to their high levels of allelic diversity and recombination[28]. Based on residual heterozygosity in the MAGIC populations, QTLs can be further validated and fine mapped through the development of Heterogeneous Inbred Families (HIFs). Selected HIFs will be isogenic at most loci in the genome, but still heterozygous for the region spanning the QTL of interest. The resulting segregating progeny will have properties similar to near-isogenic lines (hereafter named NILs) with and without the QTL of interest and are ideal genetic material to perform precise phenotyping and transcriptomic analysis, and to assess the allelic contributions to the trait of interest as well as for fine mapping and candidate causal gene identification[29].

In this study, we describe the functional validation of *WAPO1* in determining SPS in hexaploid wheat. We used two MAGIC populations across 14 site×year environments to identify two homoeologous SPS QTLs for 7AL and 7BL. Sets of contrasting NILs derived from HIFs

segregating for the QTL on 7AL were used to validate and fine map the 7AL QTL, delivering a candidate gene *WAPO-A1* and its homoeologue *WAPO-B1*. For *WAPO-A1* we observed that increased expression in the NIAB MAGIC founder parents was positively correlated with SPS in the field. Therefore, our functional validation of the *WAPO-A1* gene in hexaploid wheat used a transgenic approach in both low- and high-SPS genetic backgrounds. This transgenic overexpression approach provided functional validation in hexaploid wheat for the role of *WAPO-A1* expression level in determining the number of SPS. Furthermore, we demonstrate that the increase in SPS in the transgenic lines is not always translated into an increased number of seeds per spike and can lead to pleiotropic or compensation effects under our growing conditions. The latter highlights the need to finely balance expression levels to achieve positive effects on yield when applied in breeding.

Results

The CSIRO and NIAB MAGIC populations have a wide phenotypic spread in SPS

Twelve field trials using an 4-parent MAGIC population[30] from CSIRO were performed between 2011 and 2014 across three field sites in New South Wales, Australia (Yanco, Narrabri, Wallendbeen) and in a Greenhouse in Canberra (ACT, Australia). Two field trials using an 8-parent MAGIC population[28] from NIAB were performed in 2014 and 2015 in Cambridge, UK. Heritability of SPS across all trials and both populations was high, varying from 0.45 to 0.86 with a mean of 0.71 (Supplementary Table 1).

Both MAGIC populations showed transgressive segregation for SPS. In the 4-parent CSIRO population, recombinant inbred lines (RILs) had a mean SPS number ranging from 12.6 to 25.0 compared to 16.3 to 23.3 for the MAGIC parents. Yitpi and Chara were identified as having a reduced mean number of SPS when compared to Westonia and Baxter. On average the difference was at least one spikelet per spike between the CSIRO parents in the low and high SPS groups. The 8-parent NIAB population, RILs had mean SPS number ranging from 17.70 to 29.80 compared to 20.32 to 26.40 for the MAGIC parents. The NIAB MAGIC parents could also be broadly divided into high and low phenotype groups, with Soissons, Robigus and Brompton having a reduced SPS number compared to the other five MAGIC parents (Alchemy, Claire, Hereward, Rialto, Xi-19).

Major novel SPS loci are on chromosomes 7AL and 7BL

QTL mapping was conducted using MPWGAIM[31] with a separate univariate analysis for each trial. In total, 203 marker-trait associations (MTAs) for SPS were identified across 12 trials for the CSIRO MAGIC population and 18 MTAs for SPS were identified across 2 trials for the NIAB MAGIC population (QTL significance $p < 0.05$) (Supplementary Tables 2&3). The CSIRO MTAs cluster into ten major QTLs that are highly significant (max. $-\log10(p) > 5$) and reproducible across at least two trials. For six of the identified QTL, we were able to assign candidate genes based on previously known allelic effects of flowering pathway genes, leaving four QTL that were initially not annotated. Of these, a SPS QTL on 7AL was observed most consistently at a high significance and was chosen for further downstream analysis (Table 1).

125 ***Table 1: Overview of major SPS QTLs in the 4-parent CSIRO and the 8-parent NIAB***
126 ***MAGIC populations and the underlying candidate genes.*** QTLs for SPS from 12 trials with
127 the 4-parent CSIRO MAGIC population and two trials with the 8-parent NIAB population. QTL
128 analyses were conducted using whole genome average interval mapping using MPWGAIM[31].
129 For the NIAB MAGIC population a genetic map adapted from Gardner et al., 2016[32] was used.
130 For the CSIRO MAGIC population a previously published map was used[31]. Genetic variance
131 (%) and significance (-log10(p)) as calculated by MPWGAIM[31]. *The QTL likely associated
132 with *VRN-A1* was only observed in the CSIRO Greenhouse studies, where vernalization did
133 not occur. [$]Inferred from reported *VRN-B3* allele. Variety abbreviations: Baxter (B), Chara (C),
134 S (Soissons), W (Westonia), Y (Yitpi)

135

Chr	Genetic region (cM)		Genetic Variance (%)		Significance (-log10(p))		Studies (n)	Candidate gene	Effect
	Left	Right	Min	Max	Min	Max			
4-parent CSIRO MAGIC population									
2BS	159.29	165.35	1.6	11.8	1.94	10.9	7/12	*PPD-B1* [33]	Late allele in C increases SPS
2DS	0	9.61	15.9	30.2	22.21	38.71	5/12	*PPD-D1* [33]	Late allele in Y/B increases SPS
2DL	95.26	99.45	1.1	5.9	2	12.03	10/12	*Unknown*	
4AL	61.76	62.68	2.6	3.6	2.19	7.17	4/12	*Unknown*	
5AL	88.39	89.07	9.5	33.2	19.55	126.39	3/12*	*VRN-A1* [33]	Late allele in B increases SPS
5BL	97.75	99.74	1	4.5	1.54	9.03	7/12	*VRN-B1* [33]	Late allele in C increases SPS
5DL	131.11	152.57	1.5	8.8	2.17	17.76	8/12	*VRN-D1* [33]	Late allele in Y/C/W increases SPS
7AL	58.7	60.3	6.6	24.8	5.33	44.05	12/12	*WAPO-A1*	See Table 2
7BL	71.72	74.59	1.4	3.9	2.31	6.73	4/12	*WAPO-B1*	See Table 2
7BS	166.24	170.19	3.2	14.5	1.4	35.67	3/12	*VRN-B3* [34]	Early allele in B decreases SPS[$]
8-parent NIAB MAGIC population									
2DS	48.57	57.64	5	12.5	4.18	12.87	2/2	*PPD-D1* [33]	Early allele in S decreases SPS
7AL	257.05	257.21	19.2	33.8	42.1	66.17	2/2	*WAPO-A1*	See Table 2
7BL	144.34	144.5	1.5	1.5	2.05	2.05	1/2	*WAPO-B1*	See Table 2

136

Despite substantially different environmental conditions, the major QTL for SPS on 7AL was observed in all 12 CSIRO trials and in two NIAB trials. This indicates that this QTL was environmentally and genetically very stable (Supplementary Table 4). In the 4-parent CSIRO population, the 7AL SPS QTL defined a 5.7Mb interval between 669.7Mb and 675.4Mb on the IWGSCv1.1 assembly, with a global significance level of -log10(p)>5 across all 12 trials and mean genotypic variance explained of 13.6%. Baxter and Westonia carry the high SPS genotype, with an average increase of 1.1 spikelets per spike in the MAGIC RILs compared to the low SPS genotype (Yitpi, Chara), under these conditions. In the 8-parent NIAB population the 7AL SPS QTL defined a narrower 2.3Mb interval between 672.0Mb and 674.3Mb. In the 2014 trial, the QTL explains a remarkable 33.8% of genetic variation in SPS within the NIAB 8-way MAGIC population at a global significance level of -log10(p) 66.17. Alchemy, Claire, Hereward, Rialto, Soissons, Xi-19 all carry the high SPS genotype, with an average increase of 2.1 spikelets per spike in the MAGIC RILs compared to the low SPS genotypes (Brompton, Robigus).

In addition to the major 7AL QTL for SPS, a homoeologous SPS QTL on 7BL with a smaller effect size was also identified in both the 4-parent CSIRO and 8-parent NIAB populations (Table 1). In the 8-parent NIAB population, this second QTL is located on a 4.9Mb interval (645.3 – 650.1Mb) directly homoeologous to the 7AL QTL (-log10(p) = 2, Genetic Variance Explained (GVE) = 1.5%). Claire, Xi-19 and Soissons carry the high 7BL SPS parental genotype. Four of the 4-parent CSIRO trials also had a 7BL QTL mapping in the vicinity (642.5Mb – 655.0Mb) with Yitpi and Baxter carrying a high SPS parental genotype (-log10(p)>2.3, mean GVE = 1.5%).

Validation and fine mapping of the 7A SPS QTL using HIFs

To validate and fine-map the 7AL QTL, four Heterogenous Inbred Families (HIFs) were derived from selected F_7 RIL lines of the 4-parent CSIRO population containing heterozygosity in the QTL region. These RILs were utilized to develop sets of NILs with contrasting presence of the 7AL SPS QTL.

Four NIL pairs (F0035, F0748, F1229, and F1570) showed consistent differences in SPS between the contrasting alleles across the 7AL locus, thus validating the QTL (Figure 1A).

For two NIL pairs (F0748 and F1570) nearly all differences were statistically significant ($p < 0.05$). Because the selected NILs carried the 7AL QTL genotypes of all four founder parents, the allelic effects for each of the founders of the 4-parent CSIRO population could be determined. In addition, the SPS region was further delimited from 5.7Mb to an interval of 2.2Mb by NIL pairs F0035 and F1570 (Figure 1B).

Additional phenotyping revealed the high SPS lines in each NIL pair also showed an increase in Grain number per spike in most cases, albeit mostly insignificant, (Supplementary Figure S1) and no differences in heading date exceeding 0.5 days were observed (Supplementary Figure S2).

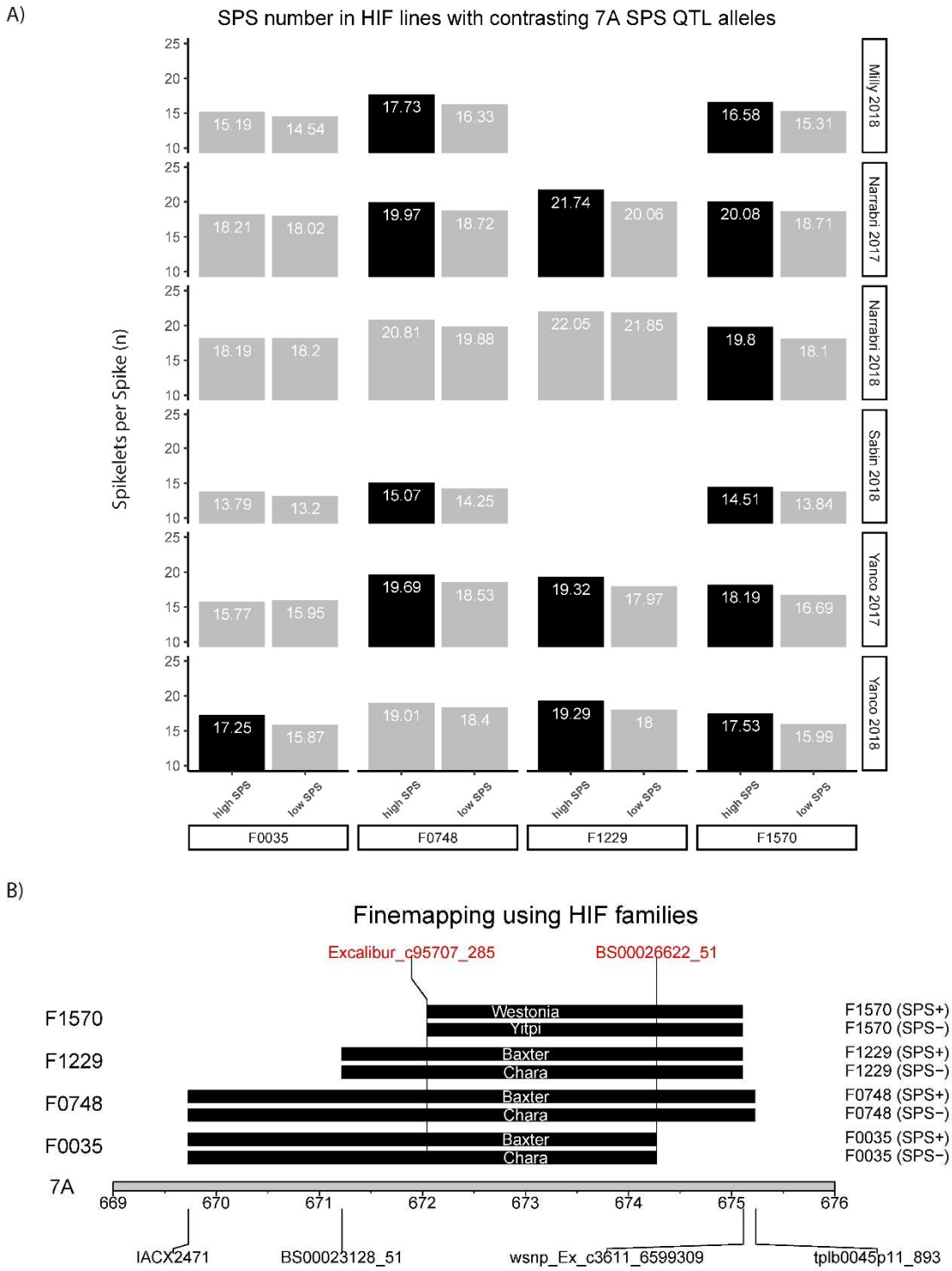

Figure 1: Validation and fine mapping of the 7A SPS QTL using HIF families derived from the CSIRO 4-way MAGIC population. A) Summary of differences in mean SPS values across NIL pairs for the 7AL SPS QTL. Black fill indicates a significant increase ($p<0.05$) between NIL pairs. B) Finemapping using HIF families. Contrasting founder genotypes in the NIL pairs are shown. The common QTL region is delimited by markers Excalibur_c95707_285 and BS00026622_51. The NIL pairs were phenotyped at four locations in France, the USA and Australia during 2017 and 2018 (6 site^{x}year combinations).

Identification of *WAPO-A1* and *WAPO-B1* as homoeologous candidate genes for SPS

The QTL region delineated using the HIFs on 7AL contained twenty genes. Both the 7AL and 7BL QTL identified in the NIAB and CSIRO MAGIC populations are syntenic to rice chromosome 6 (Figure 2). Within these three homoeologous or syntenic QTL regions, four conserved orthologous protein groups were identified*:* *TraesCS7A02G480100/TraesCS7B02G382300/OsHMA9*, *TraesCS7A02G481500/TraesCS7B02G383900/OsAAH*, *TraesCS7A02G481600/TraesCS7B02G384000/OsAPO1* and *TraesCS7A02G482000/TraesCS7B02G384200/Os06g0665100.*

OsHMA9 is a metal-efflux protein and *OsAAH* an allantoate deiminase. Neither have previously been linked to SPS phenotypes[35,36].

OsAPO1 is an F-box protein that had previously been shown to improve rice yield, primary rachis branching and lodging resistance as the causal gene of *qPBN6*[37,38] and *SCM2* QTL in rice[12]. The wheat orthologues of *OsAPO1* on 7AL and 7BL (*WAPO-A1* and *WAPO-B1*) were thus identified as good candidate genes for the 7AL and 7BL SPS QTLs. The sequences for *WAPO-A1* and *WAPO-B1* genes and *WAPO-A1* promoter sequences in Yitpi, Baxter, Chara, Westonia, Claire, Robigus, Chinese Spring and Fielder are listed in[39].

Sequence alignments showed that the high SPS *WAPO-A1* allele carries a 115bp promoter deletion and two amino acid changes (C47F and D384N). Based on recent *WAPO-A1* nomenclature[24] we reclassified our alleles accordingly (Table 2). All the assigned *WAPO-A1* alleles are consistent with the observed founder effects in both MAGIC populations for the 7AL SPS QTL.

We also classified *WAPO-B1* alleles based on recent nomenclature[22] (Table 2). All assigned *WAPO-B1* alleles are also consistent with the observed founder effects except for Soissons, which has a high SPS founder effect on 7BL, while carrying the low SPS *WAPO-B1.hap1* allele. Westonia carries the *WAPO-B1.hap3* allele, previously reported to carry a frameshift mutation/premature stop codon[22]. Based on our alignments and the protein sequence of previous WAPO-B1 gene model TRIAE_CS42_7BL_TGACv1_578478_AA1895640.1 we believe that this gene model is annotated incorrectly (Supplementary Figure S3) and that as a result, this InDel is unlikely to cause a premature stop as it falls into the 5' UTR of *WAPO-B1*. This observation would be consistent with the fact that *WAPO-B1.hap3* only has an intermediate SPS phenotype across four trials.

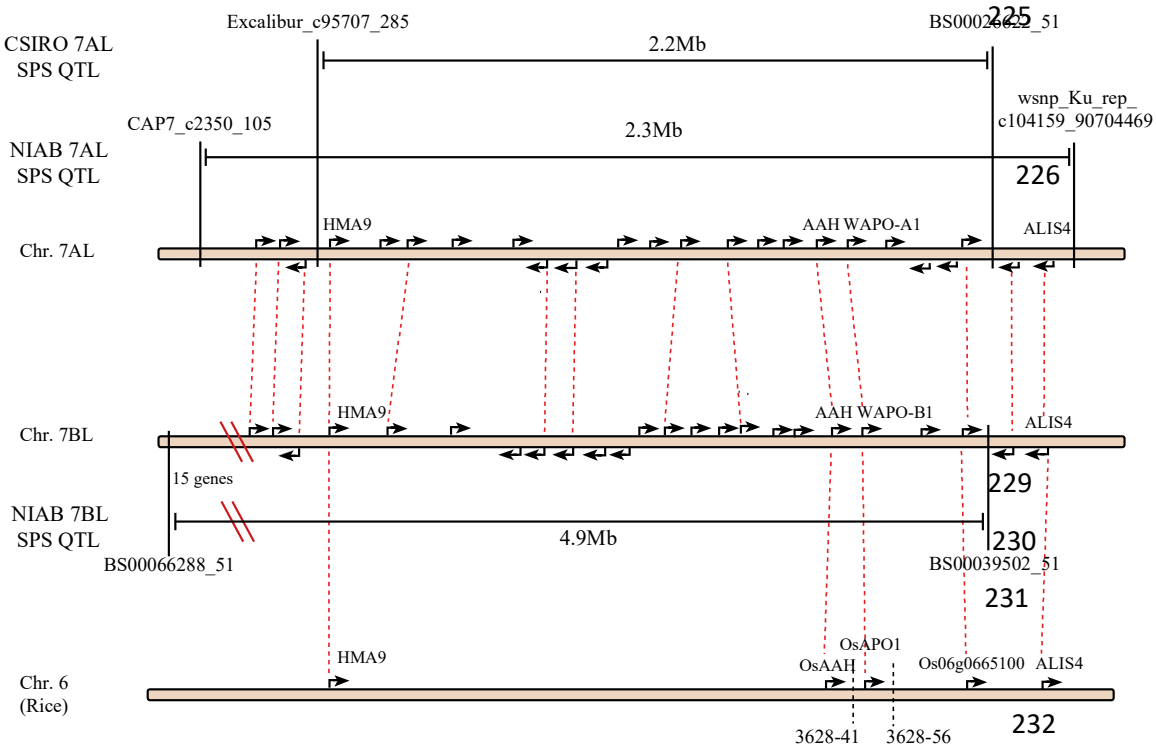

Figure 2: Syntenic relationships between the 7AL and 7BL SPS QTLs in the 4-parent CSIRO MAGIC population and the 8-parent NIAB MAGIC population and the rice SCM2/qPBN6 QTL[12,37]***.*** Arrows indicate locations of IWGSCv1.1. gene models obtained from Ensembl Plants release 51. Dashed red lines indicate homoeologous and orthologous relationships as defined by Ensembl Plants 51. Gene descriptions from Ensembl Plants 51 have been added where available. Physical distances are not drawn to scale.

240 ***Table 2: Founder effects and WAPO-A1 and WAPO-B1 alleles of NIAB and CSIRO***
241 ***MAGIC parents.***
242 Founder effects classified based on MPWGAIM predictions. *WAPO-A1* and *WAPO-B1* alleles
243 classified according to Kuzay et al., 2019[24] and Corsi et al., 2021[22]. *Founder phenotypic
244 effects for Fielder and Chinese Spring (CS) are inferred based on genome sequence
245 information since they are not MAGIC founder parents. Detailed variant calls presented in
246 Supplementary Table S5.
247

Variety	***7A SPS QTL***		***7B SPS QTL***	
	Founder effect at 7AL	***WAPO-A1* allele**	**Founder effect at 7BL**	***WAPO-B1* allele**
Yitpi	low SPS	*WAPO-A1a*	high SPS	*WAPO-B1.h2*
Baxter	high SPS	*WAPO-A1b*	high SPS	*WAPO-B1.h2*
Chara	low SPS	*WAPO-A1a*	low SPS	*WAPO-B1.h1*
Westonia	high SPS	*WAPO-A1b*	intermediate SPS	*WAPO-B1.h3*
Alchemy	high SPS	*WAPO-A1b*	low SPS	*WAPO-B1.h1*
Brompton	low SPS	*WAPO-A1a*	low SPS	*WAPO-B1.h1*
Claire	high SPS	*WAPO-A1b*	high SPS	*WAPO-B1.h2*
Hereward	high SPS	*WAPO-A1b*	low SPS	*WAPO-B1.h1*
Rialto	high SPS	*WAPO-A1b*	low SPS	*WAPO-B1.h1*
Robigus	low SPS	*WAPO-A1a*	low SPS	*WAPO-B1.h1*
Soissons	high SPS	*WAPO-A1b*	high SPS	*WAPO-B1.h1*
Xi-19	high SPS	*WAPO-A1b*	high SPS	*WAPO-B1.h2*
CS*	high SPS	*WAPO-A1b*	high SPS	*WAPO-B1.h2*
Fielder*	high SPS	*WAPO-A1b*	low SPS	*WAPO-B1.h1*

248
249
250

WAPO-A1 expression in the field is correlated with SPS

To investigate if the expression of *WAPO-A1* in wheat is correlated with SPS in the field we collected samples from tiller dissections of the eight NIAB MAGIC parents from a 2017 field nursery at growth stage GS32[40], because wheat-expression.com[41] data suggests that *WAPO1* homoeologous are expressed in the spike at this developmental stage. Expression analysis using qRT-PCR confirmed that higher *WAPO-A1* expression in wheat inflorescences is correlated (R^2 = 0.77) with increased SPS (Figure 3). The low expression of *WAPO-A1* in Soissons may be a result of the presence of the *Ppd-D1a* allele in this variety, which accelerates flowering time, so we possibly missed the expression peak of *WAPO-A1*.

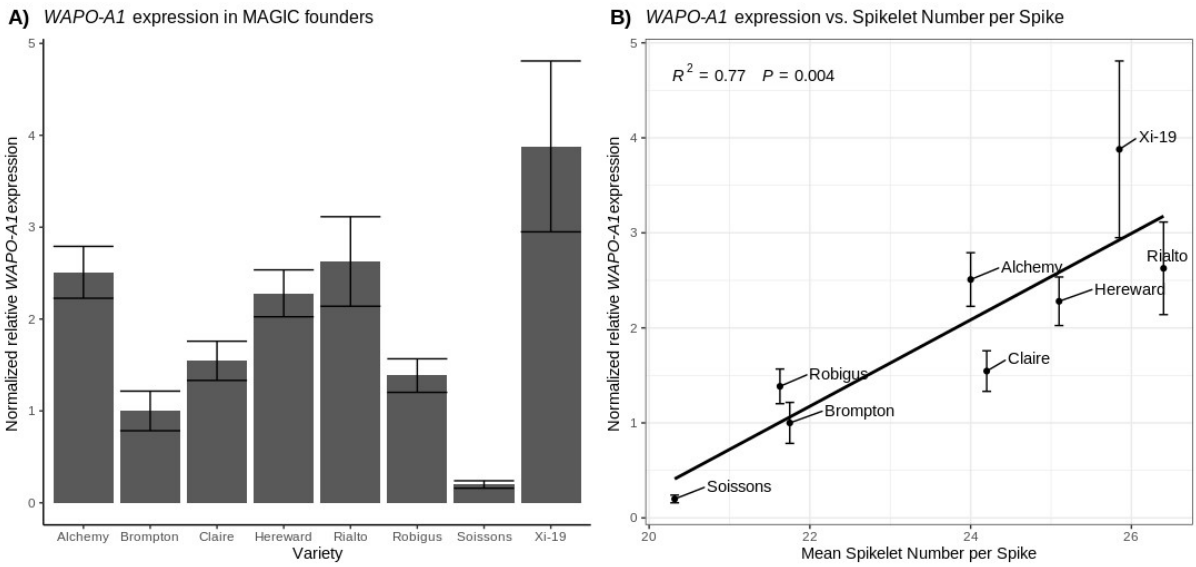

Figure 3: WAPO-A1 expression is correlated with total spikelet number. All samples were collected at GS32 apart from Soissons which at the collection date had advanced to GS34. A) Expression of *WAPO-A1* transcript relative to the housekeeping genes *TaRP15*[42] and *Ta2291*[43]and normalized to *WAPO-A1* expression in Brompton. B) Regression of expression of *WAPO-A1* (n = 3) on mean SPS for the MAGIC Founder lines (n=20) in the 2014 field trial. Error bars are SEM.

270 **Transgenic complementation of the *WAPO-A1a* allele with *WAPO-A1b* leads to**
271 **increased SPS and spike length**

272 To functionally validate the *WAPO-A1* candidate, Yitpi, carrying the low SPS *WAPO-A1a*
273 allele, was complemented with the native high SPS *WAPO-A1b* allele from Westonia using
274 Agrobacterium mediated transformation. Six sets of T_2 single-insertion homozygous lines next
275 to their respective null-segregant control line were grown in the glasshouse and phenotyped
276 (Figure 4A, 4B and Supplementary Figure S4).

277 Four out of six transgenic lines showed an increase in SPS compared to their null segregant.
278 Homozygous T_2 lines #5 and #3 displayed the strongest phenotype reaching more than 27
279 and 25 SPS, respectively, as compared to 23 in their null segregants. Homozygous plants
280 from lines #9 and #12 displayed a gain of about one SPS, while lines #4 and #7 did not show
281 a significant difference in SPS compared to their null segregants. The number of SPS in a
282 non-transformed Yitpi control was similar to the null-segregant lines (Figure 4B).

283 Samples of developing spikes at GS32 were collected from these lines for gene expression
284 analysis using qRT-PCR (Figure 4C), which revealed a strong correlation between the level
285 of *WAPO-A1* expression and the number of SPS and spike length (Figure 4D, E). These
286 results are consistent with a causal, positive correlation between *WAPO-A1* expression and
287 the number of SPS and spike length.

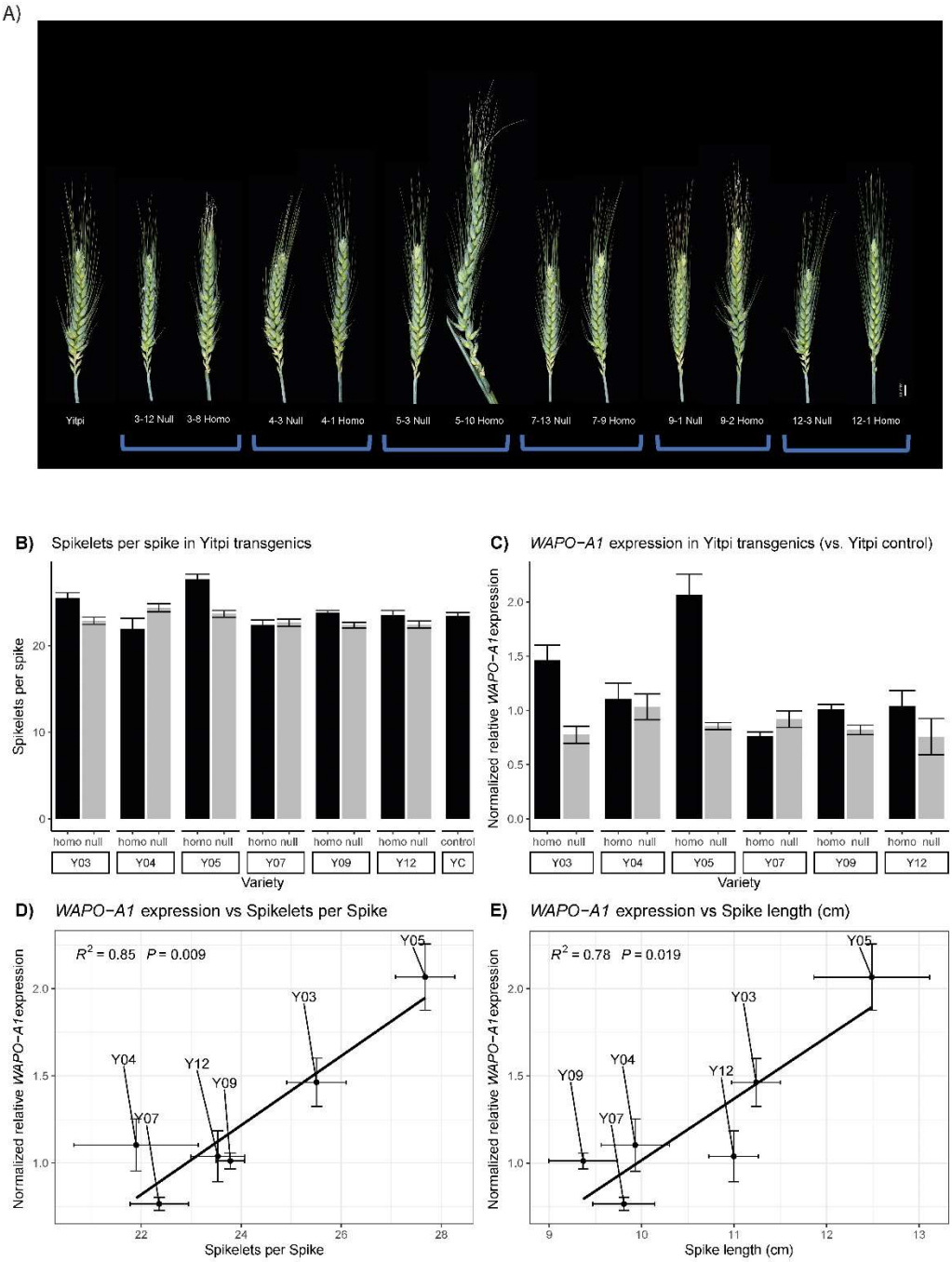

288

289 ***Figure 4: Spike phenotypes and WAPO-A1 expression in Yitpi transgenic and control***
290 ***lines.*** *A)* Representative spikes from transgenic lines, their null-segregants and non-
291 transformed Yitpi plants. We observed the appearance of infertile basal spikelets in all
292 genotypes although they were more common in transgenic plants. The presence of paired-
293 spikelets was similar across all type of plants. B) Mean SPS number phenotyped at maturity
294 in transgenic lines, their null-segregants and non-transformed Yitpi plants. C) Gene
295 expression was assayed in developing spikes dissected at GS32 and normalized to the Yitpi
296 WT control. The means and SEM of three biological replicates are shown. D) Regression of
297 expression of *WAPO-A1* on SPS for the six transgenic lines carrying the Westonia *WAPO-A1*
298 transgene. E) Regression of *WAPO-A1* expression on Spike length. For SPS and Spike
299 length, 50 spikes (5 spikes x 10 plants) of each genotype were analysed

300 **SPS levels can be increased above those conferred by the native *WAPO-A1b* allele**

301 To determine if SPS and seeds per spikelet could be increased beyond the levels of the high
302 SPS *WAPO-A1b* allele we also overexpressed the native high-SPS *WAPO-A1b* allele from
303 Westonia in Fielder, which already contains a native high-SPS *WAPO-A1b* allele. We
304 generated five independent primary transgenics in the Fielder background and isolated three
305 single-insertion lines, for which we identified homozygous T_2 and null-segregants for
306 phenotypic analysis of SPS, empty basal spikelets and seeds per spike.

307 All three transgenic lines showed an increased number of SPS in comparison to the nulls and
308 the number of SPS was strongly correlated with the level of transgene expression (Figure 5,
309 Supplementary Figure S5). These results further validated the conclusion that SPS number is
310 closely correlated with WAPO-A1 expression levels. It also demonstrates that it is possible to
311 increase SPS number beyond the levels determined by the native high SPS allele alone.

312 The Fielder control lines have fewer SPS (SPS = 17.02) than the Yitpi control (SPS = 23.44),
313 despite carrying the favourable *WAPO-A1b* allele. This difference in SPS between the two
314 cultivars could be explained by different photoperiod responses. Fielder carries the
315 photoperiod insensitive *PPD-D1a* allele while Yitpi carries the photoperiod sensitive *PPD-D1d*
316 allele, known to increase SPS[4].

317 Importantly, all the homozygous transgenic lines of Fielder, but not Yitpi containing the native
318 high SPS *WAPO-A1b* transgene had spikes displaying a "compact head" phenotype
319 (Supplementary Figure S6), which was also previously described[27]. This phenotype was
320 observed in all three Fielder families in the homozygote T_2 lines but was not seen in the null-
321 segregants.

322

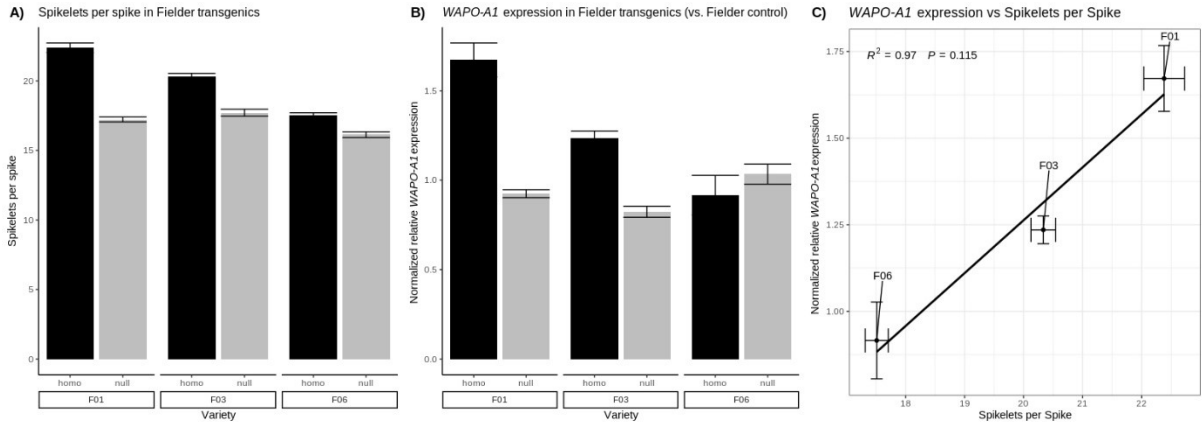

323

324 ***Figure 5: WAPO-A1 expression analysis in Fielder transgenic and control lines.*** A) Mean
325 SPS of transgenic and null-segregants of plants phenotyped at maturity; B) Gene expression
326 was assayed in developing spikes dissected at GS32. Expression is normalized to the Fielder
327 WT control. C) Regression of expression of *WAPO-A1* on SPS for the transgenic lines. Means
328 and SEM of three biological replicates are shown.

329

330

331

332

333 **Increases in *WAPO-A1* expression may cause pleiotropic effects**

334 In hexaploid wheat an increase in infertile spikelets in *WAPO-A1b* lines compared to *WAPO-*
335 *A1a* has previously been described[22,26]. In Kronos, a tetraploid wheat, a reduction in spike
336 fertility has also been reported[27], in lines containing additional WAPO-A1 transgene copies. In
337 our studies the transgenic lines with higher levels of *WAPO-A1* expression show an increased
338 number of empty basal spikelets (Supplementary Figure S7). This was especially pronounced
339 in the highest expressing lines, both in Yitpi (T_2 line #5) and Fielder (T_2 line #1). Similar to
340 phenotypes previously described in tetraploid wheat (Kronos) *WAPO-A1* overexpression
341 lines[27] we observed one or two malformed florets at the base of some spikes of the transgenic
342 lines. The phenotypic alterations are indicative for developmental disorders like homeotic
343 transformations or failed organ development (Supplementary Figure S8).

344 In rice, lines with increased *OsAPO1* expression reveal a suppression of tiller outgrowth[11].
345 Similarly, we observed a negative association between tiller number and *WAPO-A1*
346 expression across our transgenic Yitpi lines in the greenhouse pot experiment (Supplementary
347 Figure S7). However, the null segregants also showed variability in this trait meaning the
348 decrease was only significant in one line (T_2 line #5).

349 **Increased SPS in transgenic lines does not translate into equivalent increases in seed**
350 **yield**

351 Under our greenhouse conditions we could not measure a clear benefit in yield (as seeds per
352 spike or per plant) associated with transgene expression (Supplementary Figure S4), either
353 due to the pleiotropic phenotypes described above or potential source limitations under these
354 growth conditions.

355 The transgenic Yitpi line with the highest transgene expression and number of SPS (T_2 line
356 #5, T_2 line #3) showed a clear penalty in both seeds per spike and seeds per plant. We also
357 observed an extreme branching phenotype and floral defects in a small proportion of the
358 spikes developed by Yitpi T_2 line #5 (Supplementary Figure S8). In fact, the spikes were often
359 so long that they did not fully emerge from the underlying leaf sheath, and the florets inside
360 were often infertile (Figure 4A). Taken together, our data indicate, that a too high expression
361 of *WAPO-A1* reveals a rather negative effect on seed production.

362 However, lines with a lower increase of the transgene and a resulting smaller increase in SPS
363 such as Yitpi T_2 Line #12 (*WAPO-A1* expression increase 37%; Seeds per spike increase
364 11%) and Fielder T_2 line #3 (*WAPO-A1* expression increase 50%; Seeds per spike increase
365 21%) indicated that increases in seeds per spike could be observed, suggesting that one can
366 select an optimal range of *WAPO-A1* expression levels to achieve the desired phenotypic and
367 yield effects.

368

Discussion

MAGIC populations are well suited for QTL dissection

The use of two separate MAGIC populations across 14 site×year environments enabled us to capture a wide range of genetic and phenotypic variation and to identify homoeologous SPS QTL on 7AL and 7BL. The additional recombination present in MAGIC populations allowed for improved mapping resolution which aided the direct identification of candidate genes, as was the case with the NIAB MAGIC population, or via the generation of HIF lines[29]. This pipeline for candidate gene discovery via HIF lines derived from MAGIC populations is repeatable using other yield-component traits.

MAGIC populations can also reveal the effects of stacking of favourable alleles through transgressive segregation. Within the 4-parent CSIRO population alleles at the *Ppd-D1*, *PPD-B1*, *VRN-A1*, *VRN-B1* and *VRN-D1* loci are segregating in addition to *WAPO-A1* and *WAPO-B1*[30,33]. In addition to *WAPO-A1* and *WAPO-B1,* within the 8-parent NIAB population *Ppd-D1* is also segregating[4,7,28].

Overexpression of *WAPO-A1* in hexaploid wheat increases SPS

The *WAPO-A1* gene has been proposed as the candidate gene for a major QTL for SPS on 7AL mapped in several populations[22–26] and the *WAPO-B1* gene as a candidate for a smaller QTL for SPS on 7BL[22]. Recently, [27]Kuzay et al., 2022 demonstrated, using CRISPR-generated mutants and transgenic plants, the role of *WAPO-A1* and *WAPO-B1* in determining SPS in tetraploid wheat.

Here, we provide functional evidence in hexaploid wheat for a similar role of the *WAPO-A1* gene in determining SPS in a dose dependent manner. We have generated two sets of transgenic lines to test the effect on supplementing cultivars carrying either the low-SPS *WAPO-A1a* or the high-SPS *WAPO-A1b* alleles with a *WAPO-A1b* allele from a high-SPS cultivar (Westonia). In both sets of transgenic lines, we observed a positive correlation between *WAPO-A1* expression and the number of SPS, which is consistent with variation in *WAPO-A1* being responsible for the observed QTL. [27]Kuzay et al., 2022 provided strong evidence for a role of *WAPO-B1* in determining SPS, by a reduced number of SPS present in *wapo-b1* mutants. However, it was previously reported that overexpression of *WAPO-D1* in the elite hexaploid variety KN199 had no effect on spike phenotypes[19]. Different *WAPO1* homoeologues may therefore have different effects on SPS.

At the molecular level, *WAPO-A1* increases the expression of B-Class and C-Class MADS box genes, which affect lodicules, stamen and carpel development[44]. This is a possible cause behind the floral abnormalities and reduced fertility observed in both the transgenic Yitpi and Fielder lines. In the Fielder transgenics we also observed a compact spike phenotype, which indicates that the overexpression of *WAPO-A1* in these lines alters spike development in several ways. Similar phenotypes in the florets and spikes have been reported in transgenic lines overexpressing the *WAPO-A1* gene in the tetraploid wheat cv Kronos[27].

In transgenic lines displaying a low level of expression of the *WAPO-A1* transgene, and a small increase in SPS, we observed an increase in the number of seeds per spike (Yitpi line #12 and Fielder line #3). This is in line with the idea that a subtle rather than a strong increase of *WAPO-A1* expression levels could be associated with increased grain number. This is

411 similar to the situation in rice in which *SCM2*, a weaker allele of *OsAPO1* compared to *Ur1*,
412 has been reported to increase spikelet numbers without reducing panicle number[12].

413

414 ***WAPO-A1* activity is finetuned via interconnected, developmental pathways**

415 QTL mapping in two MAGIC populations also revealed large phenotypic effects of *PPD-D1a*
416 and *VRN-A1a* (and likely *VRN-B3* as well) on the number of SPS. More minor but significant
417 phenotypic effects from *PPD-B1a*, *VRN-B1a* and *VRN-D1a* were also observed. These genes
418 all influence the timing of transition from vegetative to inflorescence meristem (IM) and from
419 IM to terminal spikelet[3,4]. Where reported, later transitions are associated to increased SPS[45],
420 either linked to the duration or resources available for development. This would explain the
421 low SPS observed for Soissons, carrying the early *PPD-D1a* allele, despite having the high-
422 SPS *WAPO-A1b* allele, an observation mirrored for Fielder in comparison to Yitpi. *WAPO-A1*
423 native alleles on the other hand have not been reported to cause large changes in flowering
424 time in field trials[25,45] and while transgenic expression delayed flowering, CRISPR and EMS
425 mutants had no significant effects[27]. However, the *WAPO-A1b* allele has a larger effect on the
426 number of SPS in the winter wheat NIAB MAGIC population (+2.1 SPS) compared to the
427 spring wheat CSIRO MAGIC population (+1.1 SPS) and an epistatic interaction between
428 *WAPO-A1*, *VRN-D3*, *PPD-B1* and *Qsn.csu-6B* has been described[45]. These data together
429 support the conclusion that the phenotypic effect of *WAPO-A1* alleles on SPS is finetuned by
430 the timing of developmental transitions and the genetic constitution of *PPD1* and *VRN1.*

431 The interactions of *WAPO-A1b* with flowering pathways can also be discussed at the
432 molecular level. PPD1, *VRN1* and *VRN3*/*FT* form part of a signalling cascade that leads to the
433 upregulation of *SOC1-1* and *LFY*[46]. The orthologue of *LFY* is *OsAPO2*[47] in rice and *HvLEAFY*
434 in Barley[48], which interact with the *WAPO1* orthologues *OsAPO1* or *HvUFO* respectively.
435 OsAPO1 and OsAPO2 form a regulatory module together with LARGE2[30]. *OsAPO2* has also
436 been previously shown to be transcriptionally regulated by *SP3*[49] in rice. Together the *WAPO1*
437 pathway genes are expressed in the IM and lateral meristems and extend IM maturation and
438 control spikelet meristem identity acquisition[50]. This may also explain the extreme branching
439 phenotype observed in some spikes of the transgenic Yitpi T_2 line #5.

440 Since it could be hypothesised that particular combinations of alleles at these loci will be useful
441 to optimise grain number potential for specific environments. Given their genetic diversity, the
442 NIAB and CSIRO MAGIC populations should be an excellent tool to further study these
443 *WAPO-A1* gene network interactions and to determine how the vernalization and
444 photoperiodism genes affect *WAPO-A1* expression.

445 ***WAPO1* breeding applications**

446 Increasing SPS is a potential path to increasing seeds per spike, grain number and ultimately
447 yields. *PPD1* and *VRN1* have already been deployed to locally adapt cultivars to geographic
448 adaptation zones and due to their importance for local adaptation it can be assumed that there
449 would likely be extensive trade-offs in their use in improving SPS. *WAPO-A1b* on the other
450 hand is potentially valuable for wheat breeders as it can increase SPS in locally adapted
451 varieties without having strong impacts on flowering time.

452 However, the increased number of SPS found in most of the transgenic lines is not always
453 translated in an increased number of seeds per spike. Perhaps, under our glasshouse growing

454 conditions, the plants did not have sufficient resources to fill the extra spikelets, which might
455 be especially relevant in pot experiments, where a large number of tillers and spikes per plant
456 is formed as compared to the situation in dense canopies under field conditions. Additionally,
457 strong overexpression of *WAPO-A1* produces some defects during floret or seed
458 development.

459 These results align with those of other publications that report on the pleiotropic effects of
460 *WAPO-A1b,* including reduced spike fertility[26] and increased seeds per square meter but
461 reduced TGW[15]. As previously proposed[24], our results imply that *WAPO-A1b* promotes an
462 increase in sink capacity which may require introgression into high-biomass productive
463 varieties and cultivation under conditions that support high yield potential. The observed trade-
464 offs are not unique to *WAPO1* and have been shown in other genes that increase sink capacity
465 such as *FT2*[51] and *FUL2*[3]. In rice it has also been reported that Os*APO1* increases yield[13], but
466 that the effect on yield is source dependent[52] and dependent on gene expression levels as
467 described above.

468 It might be possible to overcome these trade-offs by stacking *OsAPO1*/*WAPO-A1* with genes
469 that have complementary phenotypic effects, and some promising examples have been
470 reported in both rice and wheat. For example, stacking *WAPO-A1* with *GNI-A1* and *qGSNP-*
471 *A-5A* to further increase SPS without reducing TGW was possible in a Japanese dihaploid
472 wheat population[14].

473 An alternative approach may be to exploit genes known to interact at the molecular level. In
474 rice it was recently shown that that OsAPO1 physically interacts with OsAPO2 and a HECT-
475 domain E3 ubiquitin ligase LARGE2/OsUPL2. LARGE2 modulates the protein stability of
476 OsAPO1 and OsAPO2[53]. Extrapolating from these results in rice, further finetuning of WAPO1
477 activity and resulting SPS and seed number might be possible in wheat through
478 posttranscriptional mechanisms and may help to overcome the constraints due to the limited
479 number of *WAPO-A1* alleles that have currently been identified.

480 **Conclusion**

481 This study has provided functional validation in hexaploid wheat for the role of *WAPO-A1* in
482 determining SPS. We demonstrated that the expression level of this gene in MAGIC lines
483 under field conditions as well as in transgenic lines in the greenhouse is positively correlated
484 with the number of spikelets per spike. We also identified potential pleiotropic effects of
485 excessive *WAPO-A1* expression. Future work can focus on identifying additional existing or
486 novel *WAPO1* alleles that have an optimized level of expression and protein activity or
487 identifying pathways and genes that can be used to optimize the expression of *WAPO1* or that
488 have complementary phenotypic effects. The optimal activity of *WAPO-A1* resulting into yield
489 gains can be expected to be dependent on the yield potential of the environment and
490 agronomic practice.

Methods

Plant Materials

The founder parents for the NIAB and CSIRO wheat MAGIC populations were selected based on wide genotypic and phenotypic diversity.

The 4-parent CSIRO MAGIC population founders are spring wheat cultivars from Australia (Yitpi, Baxter, Chara and Westonia)[30].

Six of the NIAB MAGIC population founder parents are winter wheat cultivars from the United Kingdom (UK) (Alchemy, Brompton, Claire, Hereward, Rialto, Robigus) and one from France (Soissons) and one is a facultative spring variety (Xi-19)[28].

SPS Phenotyping

For the 4-parent CSIRO MAGIC population, F_6 derived RILs were grown in partially replicated trials[54] (partial replication rate of 1.2 - 1.5): 1080 lines were grown in a Greenhouse (Canberra, ACT, Australia, CSIRO Black Mountain Site; 2011(F_9), 2012(F_{10}), 2013(F_{10})), 1009, 960 and 1008 field plots were grown in Narrabri (New South Wales, Australia; 2012(F_{10}), 2013(F_{10} & F_{11}), 2014(F_{12})), 1500, 1800 and 1009 field plots in Wallendbeen (New South Wales, Australia; 2011(F_9), 2012(F_{10}), 2013(F_{10})) and 1120, 1920 and 912 in Yanco (New South Wales, Australia; 2012(F_{10}), 2013(F_{10}), 2014(F_{12})). Three representative wheat ears were collected from each plot and the spikelets per spike (the total number of rachis nodes plus the terminal spikelet) were hand counted starting at the bottom of each spike.

Additionally, a fully replicated trial of 784 F_7 8-parent NIAB MAGIC RILs and the eight founders was grown at the NIAB experimental farm in Cambridge, UK during the 2013/2014 field season. Ten representative wheat ears were collected from 1000 of the 1600 plots in the field and dried at room temperature. Collection was done in a partially replicated design with 200 RILs and the MAGIC founders collected in duplicate. In 2014/2015 a nursery of 1091 F_8 MAGIC lines and the founders was screened for SPS as described above by collection of six representative wheat ears.

Selected F_{12}, F_{13} NIL sets were grown in 2017 and 2018 in Narrabri and Yanco, NSW, Australia and in 2018 in Sabin, Minnesota, USA and Milly-la-Forêt, France. In 2017 each line was grown in four replicates and in 2018 in six replicates. Six representative wheat ears were collected from each plot. Additional phenotyping for grains per spike was conducted in Yanco, Milly-la-Forêt and Sabin in 2018 and Heading date in Milly-la-Forêt and Sabin in 2018

QTL mapping of SPS

The 4-parent CSIRO MAGIC population had previously been genotyped using both the Infinium 9k and 90k SNP chips as well multiple DArTs and microsatellites for key genes[30,31] and the 8-parent NIAB MAGIC population using the Infinium 90k SNP chip[28,32]. QTL analyses were conducted using whole genome average interval mapping using MPWGAIM[31]. For the NIAB MAGIC population a genetic map adapted from Gardner et al., 2016[32] was used. For the CSIRO MAGIC population a previously published map was used[31]. Skimmed genetic maps containing only unique mapping locations were used to calculate MAGIC RIL haplotypes and founder probabilities, and which were then used for QTL mapping using MPWGAIM. Assigned candidate genes are based on previously published allelic information[33].

534 **Development of HIF lines and QTL fine mapping**

535 Following the process described by Barrero et al., 2015[29], four founders of heterogeneous
536 inbred families (HIFs) were identified from the F_7 MAGIC RILs through genotyping of the 7AL
537 SPS QTL region using a selection of KASP markers designed based on SNPs from the
538 Infinium iSelect 90K array [55]. After selfing of each (heterozygous) HIF founder, homozygous
539 progeny with contrasting SPS QTL genotypes were selected and self-pollinated to generate
540 sets of contrasting NILs. Plants from four families were then phenotyped across six field trials
541 as described above.

542 Genotyping of the F_{12} lines with the Infinium iSelect 90K array[55] was used to capture any
543 additional recombination in the SPS QTL region and to assign founder genotypes. All NILs
544 were checked and found to contain <1% residual heterozygosity.

545 **7AL and 7BL SPS QTL Candidate gene identification**

546 Candidate genes and their orthologues were initially identified in 2016 based on proprietary
547 gene models. Subsequently the regions have been reannotated with the IWGSCv1.1 gene
548 models as shown in Figure 2. Wheat homoeologues and rice orthologues were identified using
549 Ensembl version 51. Orthologue function was obtained through literature search and from
550 funRiceGenes[56].

551 **7AL and 7BL SPS QTL Candidate gene sequencing**

552 Publicly available *WAPO-A1* and *WAPO-B1* sequences were obtained from the reference
553 wheat line Chinese Spring[57] as well as from Brompton, Robigus and Cadenza (parent of Xi-
554 19)[58]. Additionally, full length sequences for *WAPO-A1* including 5kb upstream promoter
555 sequences in Yitpi, Baxter, Chara and Westonia were obtained via cloning and Sanger
556 Sequencing. Exome sequences for WAPO1 homoeologues in Alchemy, Claire, Hereward,
557 Rialto, Soissons and Xi-19 were obtained via Exome Capture sequencing.

558 Based on the Chinese Spring reference sequence primers were designed and *WAPO-A1*, *B1*
559 and *D1* sequences were cloned from Chinese Spring, Chara, Baxter, Westonia and Yitpi using
560 a Zero Blunt TOPO Cloning kit (Invitrogen). Subsequently the 5kb promoter sequences for
561 *WAPO-A1* were cloned from overlapping PCRs using the same methodology. Clones were
562 selected on LB + Kanamycin medium and sent for Sanger sequencing after two nights of
563 incubation at 37ºC. Sanger Sequencing was performed by LGC (UK). Sequences are available
564 as part of patent application [39]WO2019/138083. PCR conditions and primers are available in
565 Supplementary Table S6.

566 Wheat Exome Capture sequencing was conducted using a set of internal exome probes based
567 on the IWGSC RefSeqv1 annotations (pre-release) including CDS + UTR sequences. Probe
568 design and balancing was carried out by Roche. Genomic DNA was extracted using a Qiagen
569 DNeasy Mini Kit (Qiagen, US). Library preparation, sequence capture and sequencing were
570 performed at Fasteris. Sequencing was performed on an Illumina HiSeq3000 to obtain an
571 average of 8.2Gb of raw sequence data (2×150bp paired end reads) per sample. Reads for
572 the eight NIAB founders were mapped to the repeat-masked Chinese Spring reference
573 genome (IWGSCv1.0) including mitochondrial (EMBL accession: AP008982) and chloroplast
574 (EMBL accession: AB042240) genomes with BWA[59] (Li, 2013). This includes an additional
575 remapping step to fine-map InDels. Variant calling and filtering were conducted using GATK[60].
576 Data was stored and accessed through the BiofacetSNP sequence variant data management
577 system.

578

579 **Candidate gene expression analysis**

580 Chinese Spring developmental time course gene expression data from Choulet et al., 2014[61]
581 for corresponding TGACv1 gene models was accessed on wheat-expression.com[41] in March,
582 2017. As *WAPO-A1* was not annotated as part of the IWGSC_CSSv2.2[62] and TGACv1 gene
583 models[63] available B and D genome models were used as a query instead.

584 **Gene expression of *WAPO-A1* in the field**

585 Three replicates of whole spike samples were collected from tiller dissections of the 2017
586 NIAB MAGIC Nursery at growth stage GS32[40] for the MAGIC founders Alchemy, Brompton,
587 Claire, Hereward, Rialto, Robigus and Xi-19. At the collection date Soissons had advanced to
588 GS34. Following dissection, spikes were immediately frozen in liquid nitrogen. For *WAPO-A1,*
589 betaine solution was added at a final concentration of 1M to overcome the amplicons high GC
590 content. To confirm specificity of qRT-PCR reactions the melt curves for each reaction were
591 checked for the presence of only a single peak. Specificity of the assays was confirmed
592 against genomic nullitetrasomic DNA obtained from Seedstor.ac.uk (WPGS1289-PG-1,
593 WPGS1296-PG-1, WPGS1301-PG-1). Expression levels of W*APO-A1* were calculated
594 relative to the expression of the housekeeping genes *TaRP15*[42]and *Ta2291*[43]. Primers
595 sequences are in Supplementary Table S7.

596 ***WAPO-A1* Transformation experiments**

597 A 7,973 bp gene cassette containing the entire Westonia *WAPO-A1* sequence including 5.4
598 kb of the native promoter was synthetically design at GeneArt (Thermo Fischer Scientific, US)
599 and received in the standard cloning vector pUC57. This cassette was subcloned into the
600 binary vector VecBarII (using the XbaI and HindIII sites), which has been extensively used at
601 CSIRO for wheat transformation[64]. CSIRO's Transformation Unit performed the transformation
602 of the Yitpi cultivar or Fielder, using Agrobacterium[65]. Yitpi was chosen over Chara for the
603 complementation experiment because of previous work done at CSIRO showing higher
604 transformation rates in Yitpi (19-27% for Yitpi vs. 5-9% for Chara, data not shown).

605 Thirteen Yitpi and five Fielder primary transformants were generated and grown in pots in the
606 glasshouse. To assess the copy number in each primary transgenic, 25 T_1 seeds from each
607 T_0 plant were germinated in petri dishes and a Basta-resistance 'leaf assay' was used to
608 determine transgene segregation[66]. After a week, the resistance to Basta was scored to
609 determine segregation ratios (data not shown). Based on the segregation ratios six T_0 Yitpi
610 and three T_0 Fielder transformants were selected for further work. From each of them eight T_1
611 positive lines and two null-segregants were transplanted to soil and grown in glasshouse
612 conditions. For each T_1 plant, about 25 T_2 seeds were used in leaf-tipping assays to identify
613 homozygote lines. A T_2 homozygous and a null-segregant lines from each family were chosen
614 for final analysis. Ten plants of each were transplanted to pots in the glasshouse and they
615 were phenotyped at maturity. Samples were also collected for gene expression analysis in
616 developing spikes.

617 Gene expression of *WAPO-A1* in transgenic and control lines was analyzed by RT-qPCR in
618 developing spikes at GS32. Expression levels were calculated relative to the housekeeping
619 gene *TaActin1* (CJ961169). Primer sequences are in Supplementary Table S7.
620
621
622
623

Acknowledgements

CSIRO acknowledges the contributions of Dr Megan N. Hemming, Dr Alex Whan, Dr Richard A. James, Dr Sally Walford and Mr Andrew Spriggs for their support at the early stages of this project. Thanks to Ms Tracy Willis, Mr Jackson Tahapehi, Mr Alexandre Boyer, Dr Aderajew Haddis, Ms Alison Fattore, Ms Bec Maher, Mr David Lewis, Mr Max Bloomfield, Mr Mick Weiss, Mr Patrick Moody and Mr Todd Collins for the management of the field trials at CSIRO. We also thank Ms Terese Richardson and Ms Dhara Bhatt for their work at the CSIRO Wheat Transformation Unit. BASF thanks Xi Wang and Ruvini Ariyadasa for contributions to data analysis early in the work and Greta De Both, Stephanie Thepot, and David Bonnett for management of the field trials at BASF. This project was supported by BASF. Lukas Wittern was funded by BBSRC iCASE grant BB/K011790/1 awarded to Alex Webb (University of Cambridge), Matthew Hannah (BASF) and Andy Greenland (NIAB). Gareth Steed was funded by BBSRC iCASE grant BB/M015416/1 awarded to Alex Webb and Matthew Hannah.

Competing interests

Patent application [39]WO2019/138083 A1 has previously been submitted based on some of these results. John Jacobs, Mark Davey, Matthew Hannah, Claus Frohberg, Ralf-Christian Schmidt, Colin Cavanagh and Antje Rohde are employees of BASF. Gareth Steed declares no competing interest.

Data availability

The datasets generated are available for academic partners for non-commercial purposes upon request sent to the corresponding author, provided that bilateral terms-of-use agreements can be concluded.

Author contributions statements

The 4-parent CSIRO MAGIC QTL and HIF work was led by WDB and KLV. JMB and TH did the transgenic analysis. Input on design, analysis and interpretation of results was provided by AR, CC, CF, JJ, MD, MH, RCS and SS. The 8-parent NIAB MAGIC QTL work was conducted by LMW, with gene-expression analysis by LMW and GS. Input on design, analysis and interpretation of results was provided by AARW, KG and MH. LMW and JMB wrote the manuscript. All authors reviewed the manuscript.

653 **Citations**

654 1. Sreenivasulu, N. & Schnurbusch, T. A genetic playground for enhancing grain number in
655 cereals. *Trends in Plant Science* **17**, 91–101 (2012).
656 2. Zhang, J. *et al.* Identification and validation of QTL for grain yield and plant water status
657 under contrasting water treatments in fall-sown spring wheats. *Theoretical and Applied*
658 *Genetics* **131**, 1741–1759 (2018).
659 3. Li, C. *et al.* Wheat VRN1, FUL2 and FUL3 play critical and redundant roles in spikelet
660 development and spike determinacy. *Development* **146**, dev175398 (2019).
661 4. Shaw, L. M., Turner, A. S., Herry, L., Griffiths, S. & Laurie, D. A. Mutant Alleles of
662 Photoperiod-1 in Wheat (Triticum aestivum L.) That Confer a Late Flowering Phenotype
663 in Long Days. *PLOS ONE* **8**, e79459 (2013).
664 5. Brassac, J., Muqaddasi, Q. H., Plieske, J., Ganal, M. W. & Röder, M. S. Linkage
665 mapping identifies a non-synonymous mutation in FLOWERING LOCUS T (FT-B1)
666 increasing spikelet number per spike. *Scientific Reports* **11**, 1585 (2021).
667 6. Shaw, L. M. *et al.* FLOWERING LOCUS T2 regulates spike development and fertility in
668 temperate cereals. *Journal of Experimental Botany* **70**, 193–204 (2019).
669 7. Alvarez, M. A., Tranquilli, G., Lewis, S., Kippes, N. & Dubcovsky, J. Genetic and physical
670 mapping of the earliness per se locus Eps-Am1 in Triticum monococcum identifies
671 EARLY FLOWERING 3 (ELF3) as a candidate gene. *Functional & Integrative Genomics*
672 **16**, 365–382 (2016).
673 8. Brinton, J. & Uauy, C. A reductionist approach to dissecting grain weight and yield in
674 wheat. *Journal of Integrative Plant Biology* **61**, 337–358 (2019).
675 9. Li, G., Zhang, H., Li, J., Zhang, Z. & Li, Z. Genetic control of panicle architecture in rice.
676 *The Crop Journal* **9**, 590–597 (2021).
677 10. Ikeda, K., Ito, M., Nagasawa, N., Kyozuka, J. & Nagato, Y. Rice ABERRANT PANICLE
678 ORGANIZATION 1, encoding an F-box protein, regulates meristem fate. *The Plant*
679 *Journal* **51**, 1030–1040 (2007).

680 11. Ikeda-Kawakatsu, K. *et al.* Expression Level of ABERRANT PANICLE
681 ORGANIZATION1 Determines Rice Inflorescence Form through Control of Cell
682 Proliferation in the Meristem. *Plant Physiology* **150**, 736–747 (2009).
683 12. Ookawa, T. *et al.* New approach for rice improvement using a pleiotropic QTL gene for
684 lodging resistance and yield. *Nature Communications* **1**, 132 (2010).
685 13. Kim, S.-R. *et al.* Development and validation of allele-specific SNP/indel markers for
686 eight yield-enhancing genes using whole-genome sequencing strategy to increase yield
687 potential of rice, Oryza sativa L. *Rice* **9**, 12 (2016).
688 14. Mizuno, N. *et al.* Genetic mechanisms determining grain number distribution along the
689 spike and their effect on yield components in wheat. *Molecular Breeding* **41**, 62 (2021).
690 15. Ward, B. P. *et al.* Genome-wide association studies for yield-related traits in soft red
691 winter wheat grown in Virginia. *PLoS One* **14**, e0208217–e0208217 (2019).
692 16. Pang, Y. *et al.* High-Resolution Genome-wide Association Study Identifies Genomic
693 Regions and Candidate Genes for Important Agronomic Traits in Wheat. *Molecular Plant*
694 **13**, 1311–1327 (2020).
695 17. Würschum, T., Leiser, W. L., Langer, S. M., Tucker, M. R. & Longin, C. F. H. Phenotypic
696 and genetic analysis of spike and kernel characteristics in wheat reveals long-term
697 genetic trends of grain yield components. *Theoretical and Applied Genetics* **131**, 2071–
698 2084 (2018).
699 18. Boeven, P. H. G. *et al.* Genetic architecture of male floral traits required for hybrid wheat
700 breeding. *Theoretical and Applied Genetics* **129**, 2343–2357 (2016).
701 19. Wang, Y. *et al.* Transcriptome Association Identifies Regulators of Wheat Spike
702 Architecture. *Plant Physiology* **175**, 746–757 (2017).
703 20. Su, Z. *et al.* Single nucleotide polymorphism tightly linked to a major QTL on
704 chromosome 7A for both kernel length and kernel weight in wheat. *Molecular Breeding*
705 **36**, 15 (2016).

706 21. Zhai, H. *et al.* QTL Analysis of Spike Morphological Traits and Plant Height in Winter
707 Wheat (Triticum aestivum L.) Using a High-Density SNP and SSR-Based Linkage Map.
708 *Frontiers in Plant Science* **7**, 1617 (2016).
709 22. Corsi, B. *et al.* Identification of eight QTL controlling multiple yield components in a
710 German multi-parental wheat population, including Rht24, WAPO-A1, WAPO-B1 and
711 genetic loci on chromosomes 5A and 6A. *Theoretical and Applied Genetics* **134**, 1435–
712 1454 (2021).
713 23. Scott, M. F. *et al.* Limited haplotype diversity underlies polygenic trait architecture across
714 70 years of wheat breeding. *Genome Biology* **22**, 137 (2021).
715 24. Kuzay, S. *et al.* Identification of a candidate gene for a QTL for spikelet number per
716 spike on wheat chromosome arm 7AL by high-resolution genetic mapping. *Theor Appl*
717 *Genet* **132**, 2689–2705 (2019).
718 25. Muqaddasi, Q. H. *et al.* TaAPO-A1, an ortholog of rice ABERRANT PANICLE
719 ORGANIZATION 1, is associated with total spikelet number per spike in elite European
720 hexaploid winter wheat (Triticum aestivum L.) varieties. *Scientific Reports* **9**, 13853
721 (2019).
722 26. Voss-Fels, K. P. *et al.* High-resolution mapping of rachis nodes per rachis, a critical
723 determinant of grain yield components in wheat. *Theoretical and Applied Genetics* **132**,
724 2707–2719 (2019).
725 27. Kuzay, S. *et al.* WAPO-A1 is the causal gene of the 7AL QTL for spikelet number per
726 spike in wheat. *PLOS Genetics* **18**, e1009747 (2022).
727 28. Mackay, I. J. *et al.* An Eight-Parent Multiparent Advanced Generation Inter-Cross
728 Population for Winter-Sown Wheat: Creation, Properties, and Validation. *G3*
729 *Genes|Genomes|Genetics* **4**, 1603–1610 (2014).
730 29. Barrero, J. M. *et al.* Transcriptomic analysis of wheat near-isogenic lines identifies
731 PM19-A1 and A2 as candidates for a major dormancy QTL. *Genome Biology* **16**, 93
732 (2015).

733 30. Huang, B. E. *et al.* A multiparent advanced generation inter-cross population for genetic
734 analysis in wheat. *Plant Biotechnology Journal* **10**, 826–839 (2012).
735 31. Verbyla, A. P., Cavanagh, C. R. & Verbyla, K. L. Whole-genome analysis of
736 multienvironment or multitrait QTL in MAGIC. *G3 (Bethesda)* **4**, 1569–1584 (2014).
737 32. Gardner, K. A., Wittern, L. M. & Mackay, I. J. A highly recombined, high-density, eight-
738 founder wheat MAGIC map reveals extensive segregation distortion and genomic
739 locations of introgression segments. *Plant Biotechnology Journal* **14**, 1406–1417 (2016).
740 33. Cane, K. *et al.* Ppd-B1 and Ppd-D1 and their effects in southern Australian wheat. *Crop*
741 *Pasture Sci.* **64**, 100–114 (2013).
742 34. Hyles, J. E. Genome To Phenome: Diversity For Adaptation And Phenology In Wheat
743 (TRITICUM AESTIVUM L.). *Genome To Phenome: Diversity For Adaptation And*
744 *Phenology In Wheat (TRITICUM AESTIVUM L.)* (2021).
745 35. Lee, S., Kim, Y.-Y., Lee, Y. & An, G. Rice P1B-type heavy-metal ATPase, OsHMA9, is a
746 metal efflux protein. *Plant Physiol* **145**, 831–842 (2007).
747 36. Werner, A. K. *et al.* The Ureide-Degrading Reactions of Purine Ring Catabolism Employ
748 Three Amidohydrolases and One Aminohydrolase in Arabidopsis, Soybean, and Rice.
749 *Plant Physiology* **163**, 672–681 (2013).
750 37. Terao, T., Nagata, K., Morino, K. & Hirose, T. A gene controlling the number of primary
751 rachis branches also controls the vascular bundle formation and hence is responsible to
752 increase the harvest index and grain yield in rice. *Theoretical and Applied Genetics* **120**,
753 875–893 (2010).
754 38. Ando, T. *et al.* Genetic dissection and pyramiding of quantitative traits for panicle
755 architecture by using chromosomal segment substitution lines in rice. *Theoretical and*
756 *Applied Genetics* **116**, 881–890 (2008).
757 39. Davey, M. *et al.* Gene underlying the number of spikelets per spike qtl in wheat on
758 chromosome 7a. (2019). Patent: WO2019/138083
759 40. Zadoks, J. C., Chang, T. T. & Konzak, C. F. A decimal code for the growth stages of
760 cereals. *Weed Research* **14**, 415–421 (1974).

761 41. Borrill, P., Ramirez-Gonzalez, R. & Uauy, C. expVIP: a Customizable RNA-seq Data
762 Analysis and Visualization Platform. *Plant Physiology* **170**, 2172–2186 (2016).
763 42. Shaw, L. M., Turner, A. S. & Laurie, D. A. The impact of photoperiod insensitive Ppd-1a
764 mutations on the photoperiod pathway across the three genomes of hexaploid wheat
765 (Triticum aestivum). *The Plant Journal* **71**, 71–84 (2012).
766 43. Paolacci, A. R., Tanzarella, O. A., Porceddu, E. & Ciaffi, M. Identification and validation
767 of reference genes for quantitative RT-PCR normalization in wheat. *BMC Molecular*
768 *Biology* **10**, 11 (2009).
769 44. Kong, X. *et al.* The wheat AGL6-like MADS-box gene is a master regulator for floral
770 organ identity and a target for spikelet meristem development manipulation. *Plant*
771 *Biotechnology Journal* **20**, 75–88 (2022).
772 45. Andrew Katz *et al.* Identification and Validation of a QTL for Spikelet Number on
773 Chromosome Arm 6BL of Common Wheat (Triticum Aestivum L.). *Molecular Breeding*
774 (2021) doi:10.21203/rs.3.rs-769537/v1.
775 46. Pearce, S., Vanzetti, L. S. & Dubcovsky, J. Exogenous Gibberellins Induce Wheat Spike
776 Development under Short Days Only in the Presence of VERNALIZATION1. *Plant*
777 *Physiology* **163**, 1433–1445 (2013).
778 47. Ikeda-Kawakatsu, K., Maekawa, M., Izawa, T., Itoh, J.-I. & Nagato, Y. ABERRANT
779 PANICLE ORGANIZATION 2/RFL, the rice ortholog of Arabidopsis LEAFY, suppresses
780 the transition from inflorescence meristem to floral meristem through interaction with
781 APO1. *The Plant Journal* **69**, 168–180 (2012).
782 48. Selva, C. *et al.* HvLEAFY controls the early stages of floral organ specification and
783 inhibits the formation of multiple ovaries in barley. *The Plant Journal* **108**, 509–527
784 (2021).
785 49. Huang, Y., Bai, X., Luo, M. & Xing, Y. Short Panicle 3 controls panicle architecture by
786 upregulating APO2/RFL and increasing cytokinin content in rice. *Journal of Integrative*
787 *Plant Biology* **61**, 987–999 (2019).

788 50. Koppolu, R., Chen, S. & Schnurbusch, T. Evolution of inflorescence branch
789 modifications in cereal crops. *Current Opinion in Plant Biology* **65**, 102168 (2022).
790 51. Glenn, P. *et al.* Identification and characterization of a natural polymorphism in FT-A2
791 associated with increased number of grains per spike in wheat. *Theoretical and Applied*
792 *Genetics* (2021) doi:10.1007/s00122-021-03992-y.
793 52. Nakano, H. *et al.* Quantitative trait loci for large sink capacity enhance rice grain yield
794 under free-air CO2 enrichment conditions. *Scientific Reports* **7**, 1827 (2017).
795 53. Huang, L. *et al.* The LARGE2-APO1/APO2 regulatory module controls panicle size and
796 grain number in rice. *The Plant Cell* **33**, 1212–1228 (2021).
797 54. Cullis, B. R., Smith, A. B. & Coombes, N. E. On the design of early generation variety
798 trials with correlated data. *Journal of Agricultural, Biological, and Environmental*
799 *Statistics* **11**, 381 (2006).
800 55. Wang, S. *et al.* Characterization of polyploid wheat genomic diversity using a high-
801 density 90,000 single nucleotide polymorphism array. *Plant Biotechnol J* **12**, 787–796
802 (2014).
803 56. Yao, W., Li, G., Yu, Y. & Ouyang, Y. funRiceGenes dataset for comprehensive
804 understanding and application of rice functional genes. *GigaScience* **7**, gix119 (2018).
805 57. IWGSC *et al.* Shifting the limits in wheat research and breeding using a fully annotated
806 reference genome. *Science* **361**, eaar7191 (2018).
807 58. Walkowiak, S. *et al.* Multiple wheat genomes reveal global variation in modern breeding.
808 *Nature* **588**, 277–283 (2020).
809 59. Li, H. W. Aligning sequence reads, clone sequences and assembly contigs with BWA-
810 MEM. *arXiv: Genomics* (2013).
811 60. McKenna, A. *et al.* The Genome Analysis Toolkit: a MapReduce framework for analyzing
812 next-generation DNA sequencing data. *Genome Res* **20**, 1297–1303 (2010).
813 61. Choulet Frédéric *et al.* Structural and functional partitioning of bread wheat chromosome
814 3B. *Science* **345**, 1249721 (2014).

815 62. IWGSC *et al.* A chromosome-based draft sequence of the hexaploid bread wheat
816 (Triticum aestivum) genome. *Science* **345**, 1251788 (2014).
817 63. Clavijo, B. J. *et al.* An improved assembly and annotation of the allohexaploid wheat
818 genome identifies complete families of agronomic genes and provides genomic evidence
819 for chromosomal translocations. *Genome Res* **27**, 885–896 (2017).
820 64. Richardson, T., Thistleton, J., Higgins, T. J., Howitt, C. & Ayliffe, M. Efficient
821 Agrobacterium transformation of elite wheat germplasm without selection. *Plant Cell,*
822 *Tissue and Organ Culture (PCTOC)* **119**, 647–659 (2014).
823 65. Ishida, Y., Tsunashima, M., Hiei, Y. & Komari, T. Wheat (Triticum aestivum L.)
824 Transformation Using Immature Embryos. in *Agrobacterium Protocols: Volume 1* (ed.
825 Wang, K.) 189–198 (Springer New York, 2015). doi:10.1007/978-1-4939-1695-5_15.
826 66. Jacobsen, J. *et al.* Barley (Hordeum vulgare L.). in *Agrobacterium Protocols* (ed. Wang,
827 K.) 171–184 (Humana Press, 2006). doi:10.1385/1-59745-130-4:171.
828

829 **Appendix**

830

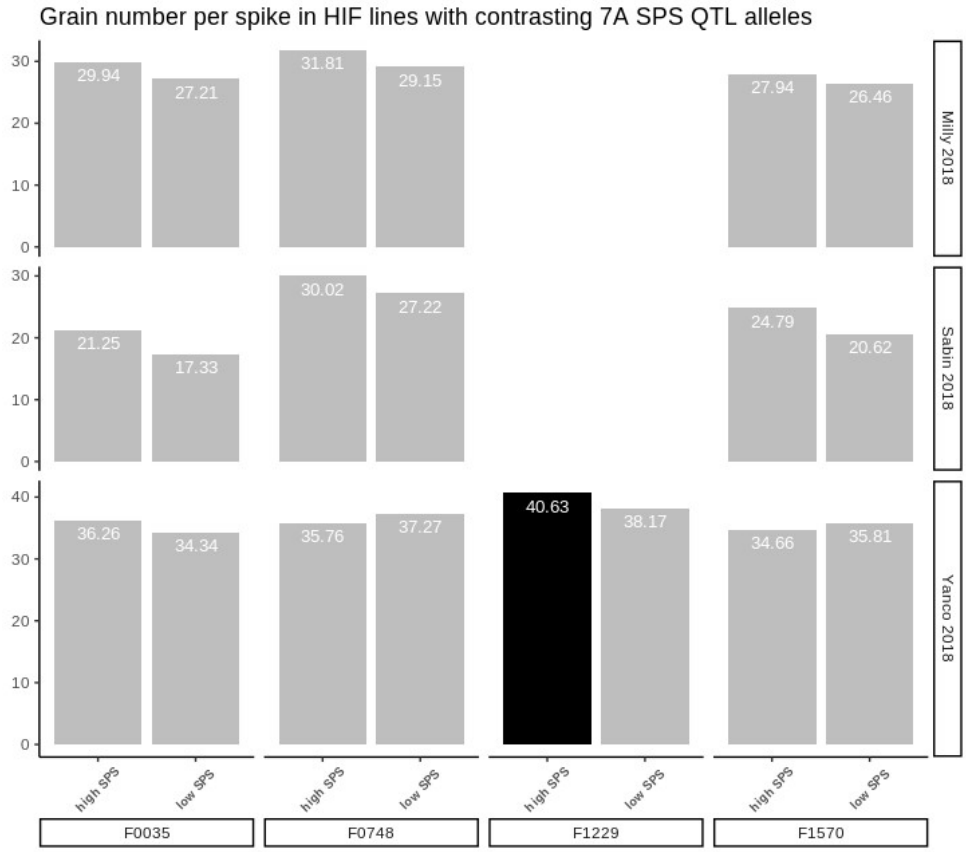

831

832

833 ***Supplementary Figure S1: Validation of phenotypes for 7AL SPS QTL using HIF***
834 ***families.*** A) Summary of differences in grain number per spike across NIL pairs for the 7AL
835 SPS QTL. Black fill indicates a significant increase ($p < 0.05$) between NIL pairs.

836

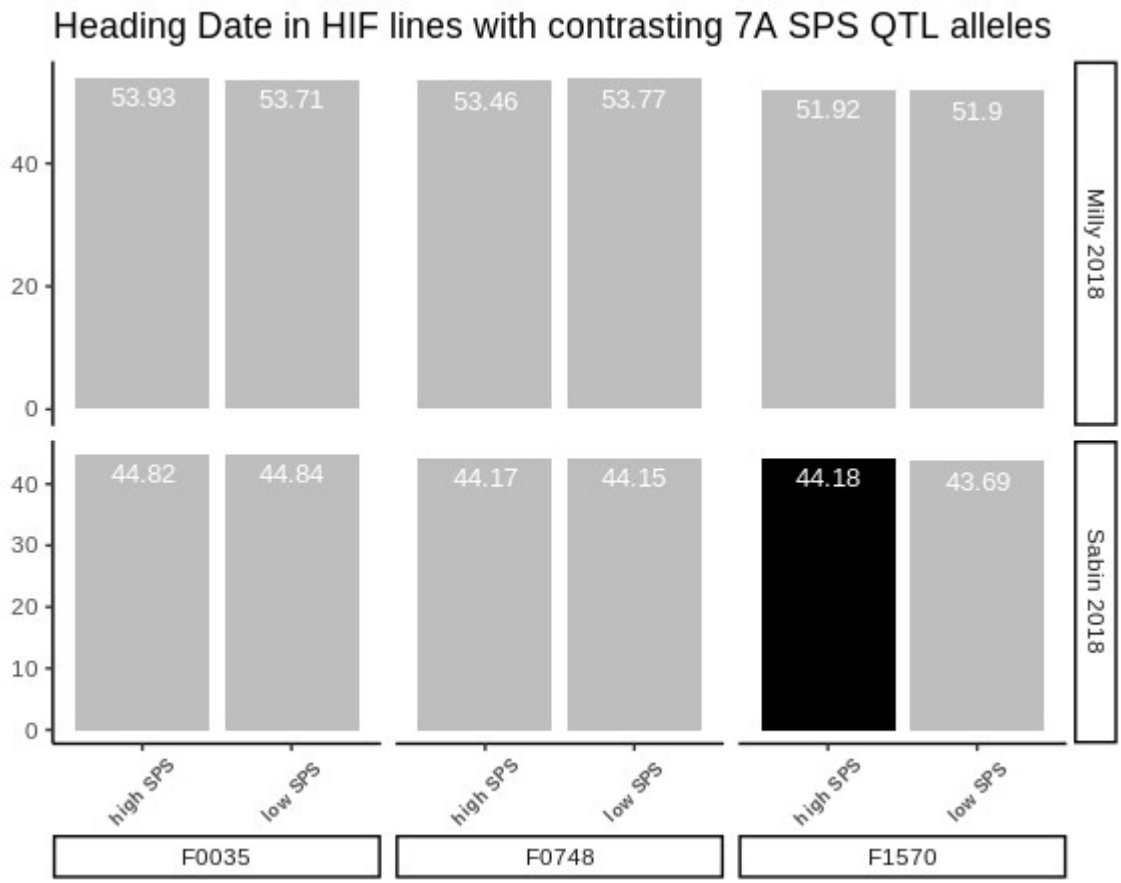

Supplementary Figure S2: Validation of phenotypes for 7AL SPS QTL using HIF families. A) Summary of differences in heading date across NIL pairs for the 7AL SPS QTL. Black fill indicates a significant increase ($p<0.05$) between NIL pairs.

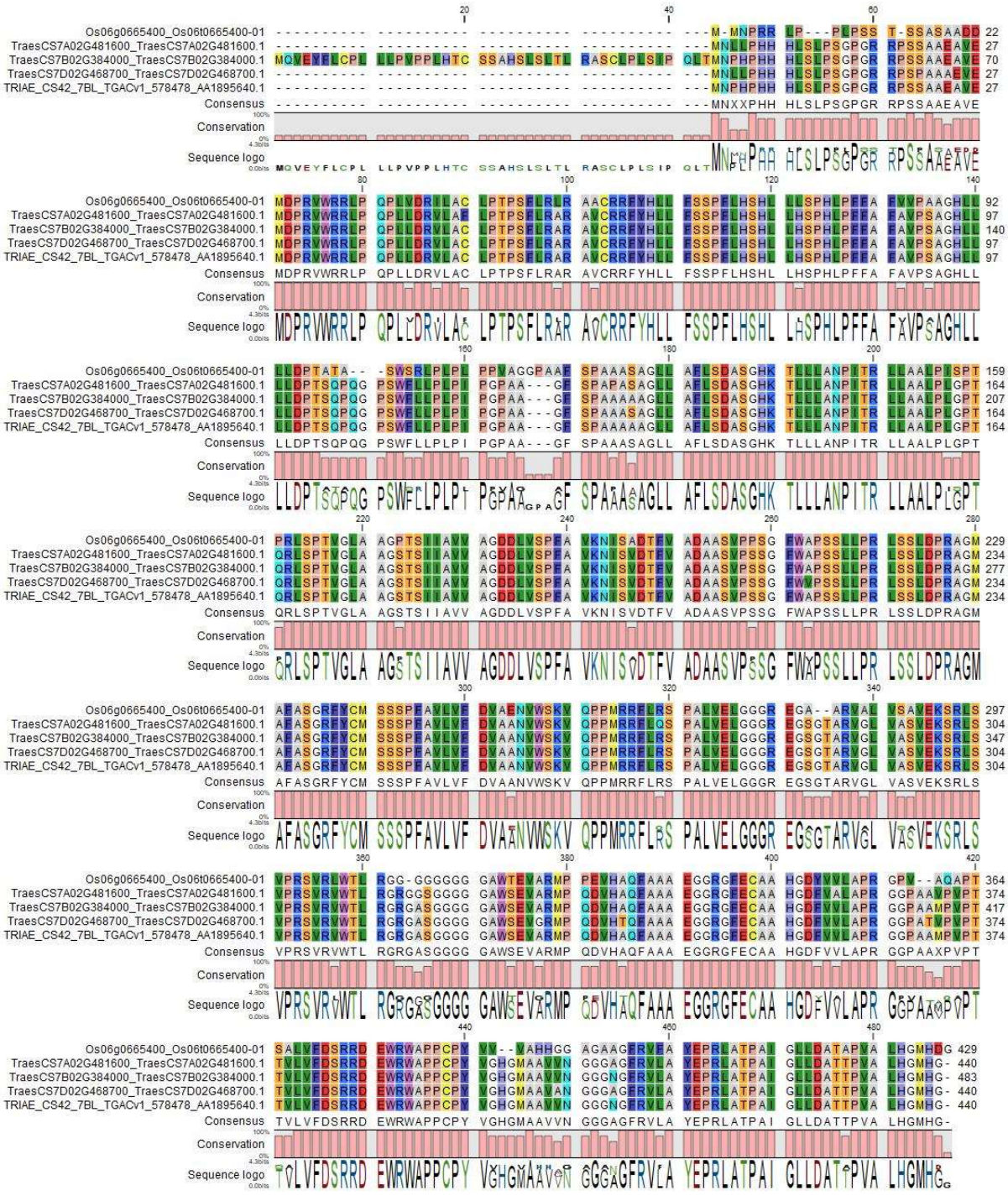

Supplementary Figure S3: **Alignment of *WAPO1* homoeologues and *OsAPO1* (*Os06g0665400*).** MCoffee alignment visualised in CLC Genomics Workbench. Amino acids coloured based on RasMol colour scheme. Amino acid % identity conservation between *WAPO-A1* and *OsAPO1* is 80%. The alternative gene model for *WAPO-B1* is *TRIAE_CS42_7BL_TGACv1_578478_AA1895640.1.*

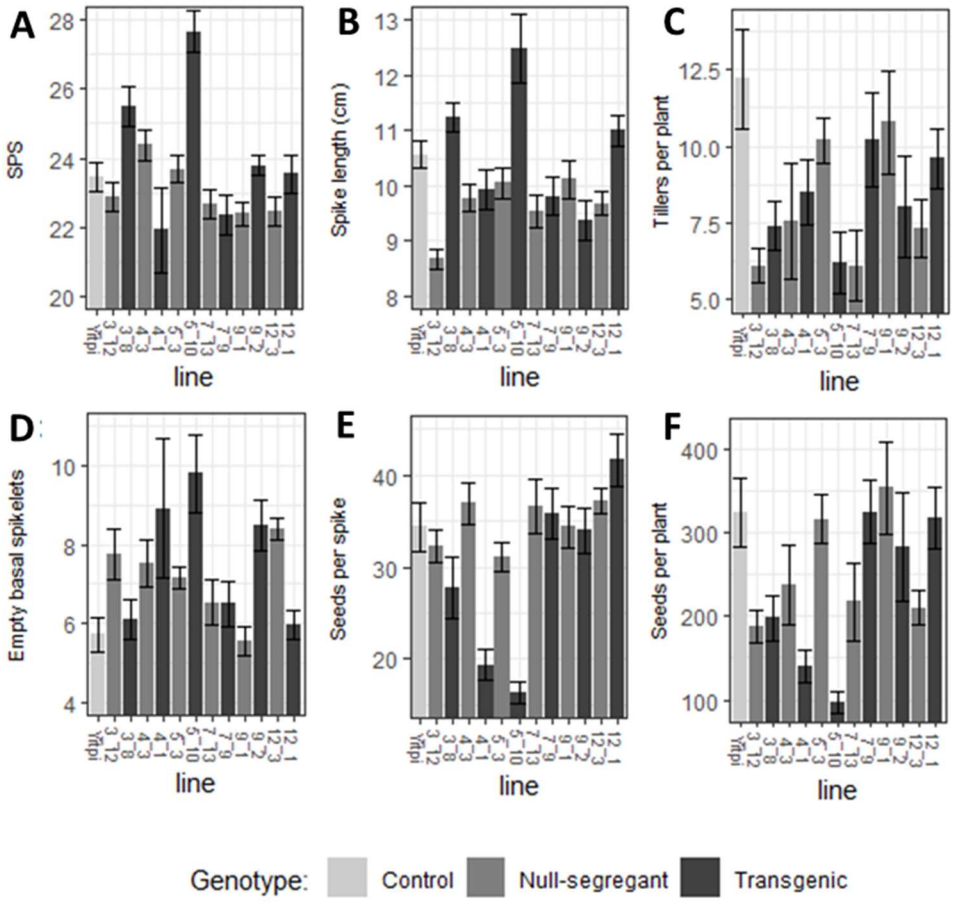

Supplementary Figure S4: Phenotypic characterisation of Yitpi transgenic, null-segregates and control spikes and plants. *A) SPS number. B) Spike length. C) Tiller number per plant. D) Empty basal spikelets. E) Seeds per spike. F) Number of seeds per plant. Means with SEM are represented.* For spike traits, 50 spikes (5 spikes x 10 plants) of each genotype were used in the calculations. Note variation in range for Y axes.

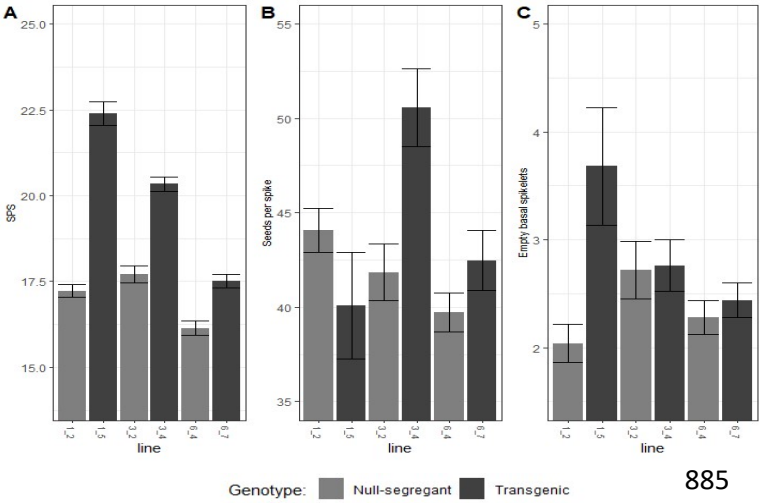

Supplementary Figure S5: Spike phenotype of transgenic Fielder plants and null-segregants. A) SPS. B) Seeds per spike. C) Empty basal spikelets. Means with SEM are shown. 50 spikes (5 spikes x 10 plants) of each genotype were used in the calculations.

Supplementary Figure S6: Examples of compact spike phenotype and of basal floret defects in Fielder transgenics. A) Fielder control spike. B-D) Examples of compact heads in over-expression lines. E) Details of homeotic floral defect in basal florets.

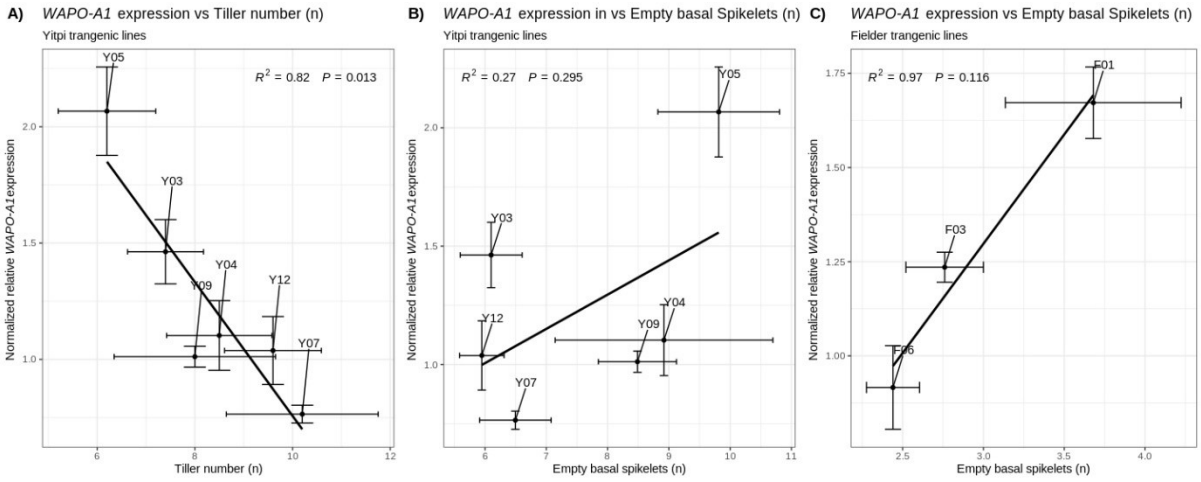

Supplementary Figure S7: Effect of WAPO-A1 expression on Tiller number and Empty basal spikelets. Gene expression was assayed in developing spikes dissected at GS32. A) Regression of normalized expression of *WAPO-A1* on Tiller number measured in Yitpi transgenic lines. B) Regression of normalized expression of *WAPO-A1* on Empty Basal Spikelets measured in Yitpi transgenic lines. C) Regression of normalized expression of *WAPO-A1* on Empty Basal Spikelets measured in Fielder transgenic lines. Means and SEM of three biological replicates are shown.

Supplementary Figure S8: Examples of branching spikes and floral defects in transgenic line 5-10. A-B) Extreme branching phenotype. C) Details of homeotic floral defect in basal florets